

### Chief Editor

Dr. A. Singaraj, M.A., M.Phil., Ph.D.

### Editor

Mrs.M.Josephin Immaculate Ruba

### EDITORIAL ADVISORS

1. Prof. Dr.Said I.Shalaby, MD,Ph.D.  
Professor & Vice President  
Tropical Medicine,  
Hepatology & Gastroenterology, NRC,  
Academy of Scientific Research and Technology,  
Cairo, Egypt.
2. Dr. Mussie T. Tessema,  
Associate Professor,  
Department of Business Administration,  
Winona State University, MN,  
United States of America,
3. Dr. Mengsteab Tesfayohannes,  
Associate Professor,  
Department of Management,  
Sigmund Weis School of Business,  
Susquehanna University,  
Selinsgrove, PENN,  
United States of America,
4. Dr. Ahmed Sebihi  
Associate Professor  
Islamic Culture and Social Sciences (ICSS),  
Department of General Education (DGE),  
Gulf Medical University (GMU),  
UAE.
5. Dr. Anne Maduka,  
Assistant Professor,  
Department of Economics,  
Anambra State University,  
Igbariam Campus,  
Nigeria.
6. Dr. D.K. Awasthi, M.Sc., Ph.D.  
Associate Professor  
Department of Chemistry,  
Sri J.N.P.G. College,  
Charbagh, Lucknow,  
Uttar Pradesh. India
7. Dr. Tirtharaj Bhoi, M.A, Ph.D,  
Assistant Professor,  
School of Social Science,  
University of Jammu,  
Jammu, Jammu & Kashmir, India.
8. Dr. Pradeep Kumar Choudhury,  
Assistant Professor,  
Institute for Studies in Industrial Development,  
An ICSSR Research Institute,  
New Delhi- 110070, India.
9. Dr. Gyanendra Awasthi, M.Sc., Ph.D., NET  
Associate Professor & HOD  
Department of Biochemistry,  
Dolphin (PG) Institute of Biomedical & Natural  
Sciences,  
Dehradun, Uttarakhand, India.
10. Dr. C. Satapathy,  
Director,  
Amity Humanity Foundation,  
Amity Business School, Bhubaneswar,  
Orissa, India.



ISSN (Online): 2455-7838

SJIF Impact Factor (2017): 5.705

EPRA International Journal of

# Research & Development (IJRD)

Monthly Peer Reviewed & Indexed  
International Online Journal

Volume:2, Issue:11, November 2017



Published By :  
EPRA Journals

CC License





# COMPOSITE TRANSMISSION OVER LARGE-CORE POLYMER OPTICAL FIBERS FOR IN-HOME NETWORKING

Jomma Prathap<sup>1</sup>

<sup>1</sup>Viswa Bharathi College of Engineering, Nizampet road Kukatpally, Hyderabad, Telangana State, India.

Ramavath Janu<sup>2</sup>

<sup>2</sup>Sree Datta College of Science and Technology, Ibrahimpatnam, Telangana State, India.

## ABSTRACT

To deliver multiple services over a single optical infrastructure, a novel composite transmission approach is proposed for an in-home access network combining multi-band (MB) discrete-Fourier-transform spread (DFT-S) discrete multi-tone (DMT) and M-ary position phase shift keying modulation (MPPSK). Bit-loading algorithm is introduced to maximize the total bit rate and permits a spectral coexistence between the two schemes. In addition, the optimal used bandwidth and multi-band number are investigated in order to maintain strong robustness against fiber nonlinearity while achieving reduced peak-to-average power ratio (PAPR). A composite DMT and two MPPSK channels over 50 m step-index (SI) polymer optical fiber (POF) link has been successfully implemented. The results demonstrate that a total bit rate of 1.122 Gbps with a bit error rate (BER) of  $1.2019 \times 10^{-4}$  and  $2.01 \times 10^{-3}$  for DMT and MPPSK are achieved respectively, and what's more, excellent coexistence performance is obtained in the composite transmission. It is a promising technique for future in-home networkings.

**KEYWORDS:** Fiber optical communication; composite transmission; MPPSK; DFT spread; In-home networks

## I. INTRODUCTION

The solution combining different transport media to deliver different wired and wireless services such as coaxial cable for video streaming, CAT-5 cable for computer data and twisted pair for wired telephony and web-browsing, is mostly used in home-access networking scenario thus lead to high complexity of network infrastructures and expensive service costs [1]. Therefore, transporting the converged multiple wired and wireless services over the same infrastructure can reduce the maintenance costs and are suitable for optical home networking [2-4]. The backbone of single mode silica optical fiber owns high capacity and is considered to be future-proof. However, the installation and maintenance costs, which are unsustainable for users, limit its application in short range transmissions.

Large core diameter ( $\phi$  1mm) Step-Index (SI) Polymer Optical Fibers (POFs), owing the advantages of low cost, easy installation, low complexity and bend insensitivity, are proposed as one of the excellent cost-effective medium and become popular in short range networking scenarios [5-6]. However, the conventional standard SI-POF provides a low bandwidth-distance product due to its mode dispersion and large numerical aperture which greatly degrades the system

capacity. Several previous works have already been experimentally shown that the bandwidth defects of SI-POF can be compensated by the advanced modulations and electronic equalization techniques [7-8]. Therefore, employing the advanced techniques to approach the channel capacity in SI-POF transmission links with intensity modulation and direct detection (IM/DD) structure gains significant attentions and researches [9-12]. Discrete multi-tone (DMT) modulation, similar to orthogonal frequency division multiplexing (OFDM), is a baseband version of the multi-carrier modulation technique which has been widely used in Digital Subscriber Line (DSL) systems. The M-ary Position Phase Shift Keying (MPPSK), commonly used in wireless communication system, is a kind of bandwidth-efficient modulations and can be well demodulated even in a very low signal-to-noise ratios (SNRs) environment with low power cost.

In this paper, a composite transmission, combining DMT and MPPSK in separated frequency bands, over a single SI-POF link is investigated. This is a new delivery scheme of multiple services over in-home access network to bring down the cost of the civil works as well as increased revenues. The main goal of this paper is to try to apply the novel hybrid modulation format over IM/DD SI-POF transmission links. Section II describes optical communication over POF with the IM/DD structure. In section III, a novel composite transmission diagram is proposed. The multi-band (MB) DFT-spread (DFT-S) technique is introduced to make use of the character domain and reduce the peak-to-average power ratio (PAPR). Section IV outlines the results and discussions, where the DMT signal occupied (0-236) MHz and two adjacent MPPSK channels centered at 250MHz and 260MHz over POF transmission are analyzed. Section V gives the conclusions.

## II. IM/DD COMMUNICATION OVER SI-POF

The IM/DD structure, which only light intensity is modulated, is usually adopted in SI-POF transmission systems under a low-cost consideration [11]. An electrical modulator is used to convert the information data into the original bipolar signal and a DC bias current is usually added in order to generate a positive unipolar signal that will be used to drive the electrical-to-optical (E-O) component. Hence, the electrical signal directly modulates the power intensity of the optical signal. After SI-POF transmission, the received optical signal is

detected by photodetector and its power intensity is converted into electrical current and then demodulated in the electrical domain accordingly.

In this paper, the standard 1 mm core polymethyl metacrylate (PMMA) SI-POF, standardized by the IEC in 2008 as A4a.2 POF, is adopted and investigated. Based on the measurements [12][13], the transmission channel can be modeled as a Gaussian low-pass filter and the normalized frequency response is expressed as:

$$|H(f)|^2 = \exp\left\{-\left[\frac{f}{f_0}\right]^2\right\} \quad (1)$$

where  $f_0 = \frac{f_{3dB}}{\sqrt{\ln 2}}$ ,  $f_{3dB}$  is the -3dB bandwidth.

**III. THE COMPOSITE TRANSMISSION SCHEME**

According to the low-pass property of the SI-POF channel, the transmission region can be divided into two frequency domains with high SNR and low SNR respectively. The low SNR region is not suitable for DMT transmission with the bit error rate (BER) considerations thus that spectrum is wasted. Owing to the low power cost and excellent demodulation performance of MPPSK, DMT and MPPSK signals in different frequency bands can be combined to convey multiple services simultaneously. A block diagram of the composite transmission scheme is designed as in Fig. 1.

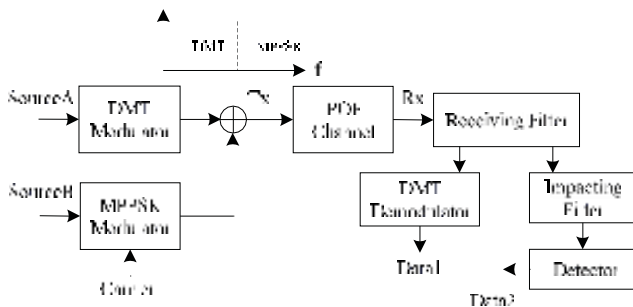


Fig. 1. The composited transmission scheme.

**A. MPPSK**

Due to small angle phase transition intervals are adopted in MPPSK modulation, the spectrum of the transmitting signal is tightened and a very high spectral efficiency can be obtained. Let  $G_k (k = 0, 1, \dots, M_0 - 1)$  be the modulated symbol, the samples  $f_0(t)$  and  $f_k(t)$ , associated with logical '0' and logical 'k' respectively, are designed for the followings:

$$f_0(t) = A \sin 2\pi f_c t, \quad 0 \leq t < T \quad (2)$$

$$f_k(t) = \begin{cases} A \sin 2\pi f_c t, & 0 \leq t < (k-1)T \\ B \sin(2\pi f_c t + \theta), & (k-1)T \leq t < kT \\ A \sin 2\pi f_c t, & kT \leq t < T \end{cases} \quad (3)$$

where  $T = N_0 T_C$  is the symbol width,  $\theta$  is the modulating angle,  $T_C = 1/f_c$  is the carrier cycle,  $\mathbf{1} = K T_C$  is the temporal length of carrier cycles with phase transition,  $A$  and  $B$  are the amplitude of modulated waveforms. It can be seen that the classical binary phase shift keying (BPSK) modulation is the special case of (2) and (3) on the condition that  $\mathbf{1} = T$ ,  $\theta = \pi$  and  $M_0 = 2$ . The received MPPSK signal can be easily recovered by using a special impacting filter (SIF) and envelope detector even in the low SNR condition.

**B. Multi-band DFT-Spread DMT**

One of the intrinsic disadvantages of the conventional DMT is high PAPR which would degrade the system performance. In order to deal with the PAPR problem, spreading techniques, namely DFT-S, have been proposed in the DMT transmission over a short range POF link [14][15]. However, it is worth noting that the spread symbols are distributively mapped across the whole DMT spectrum, thus the PAPR are rapidly modified by the large POF dispersion when delivering a long distance so that the low PAPR advantage at the transmitter will be negated and the PAPR reduction is not effective. It is a fact that DFT-S DMT signal is sensitive to non-linearity distortion in POF systems and then requires a robust equalizer at the receiver, which will increase the complexity of the whole system. Therefore, an improved DFT-S DMT scheme with split symbol-spread blocks is adopted to strengthen the robustness against fiber nonlinearity.

Fig. 2 demonstrates the conceptual diagram of baseband MB-DFT-S DMT modulator with sub-band mapping. The bit-loading algorithm is also adopted in the practical transmission so as to maximize the total data rate with a symbol error rate (SER) target. As shown in the Fig. 2, the entire spectrum of DMT is split into  $L$  bands with  $M$  sub-carriers per sub-band which can be assigned with different modulation orders based on the sub-channel SNR.

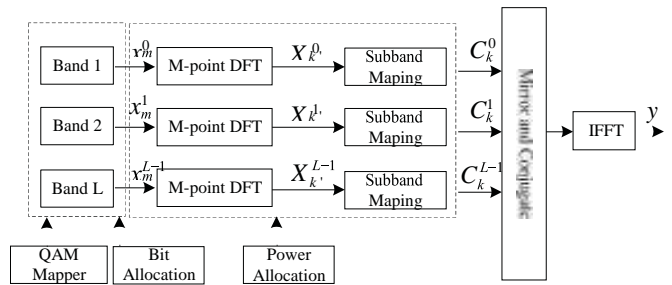


Fig. 2. Block diagram of a MB-DFT-S DMT modulator.

Assuming there are  $N$  carriers, where  $N = M \cdot L$ ,  $x_m^l$  ( $l = 0, \dots, L-1, m = 0, \dots, M-1$ ), is the  $(m + 1)$ th data symbol in the  $(l + 1)$ th band. Contrary to the conventional DMT, the original symbol  $x_m^l$  is precoded by a  $M$  point DFT block firstly. Then, a new set of  $M$  symbols is generated by:

$$X_k^l = \sum_{m=0}^{M-1} x_m^l e^{j \frac{-2\pi m k'}{M}}, \quad k' = 0, \dots, M-1 \quad (4)$$

$X_{k'}^l$  are then sub-band mapped onto  $N$  point DFT symbol vector  $C = \{C_k^0, \dots, C_k^1, \dots, C_k^{L-1}\}$  where  $C_k^l$  can be expressed as:

$$C_k^l = \begin{cases} X_{k'}^l & k = k' + Ml \\ 0 & \text{others} \end{cases}, k = 0, \dots, N-1 \quad (5)$$

After the mirror and conjugate processing and IFFT computation, the time domain signals are illustrated as:

$$y(k) = \frac{1}{\sqrt{2N}} \sum_{n=0}^{2N-1} C_k^l \exp(j2\pi nk/2N), k = 0, 1, \dots, 2N-1 \quad (6)$$

$$C_{2N-k}^l = (C_k^l)^* \quad (7)$$

where  $C_k^l$  following the Hermitian symmetry property given in (7), is the complex value according to the sub-band constellation mapping. Simply to say, the modulated MB-DFT-S DMT signals can be represented as followings:

$$y = IDFT \{0, C_k^0, \dots, C_k^{L-1}, null, (C_k^{L-1})^*, \dots, (C_k^0)^*\} \quad (8)$$

On the receiver side, the demodulation process, designed as in Fig. 3, is the reverse of equation (4), (5) and (8).

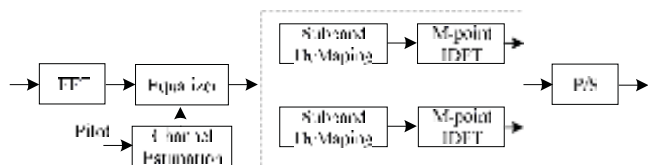


Fig. 3. Block diagram of a MB-DFT-S DMT receiver.

Assuming the additive white Gaussian noise in POF system is equally allocated for each sub-channel,  $E_m^l$  is the allocated power of the  $(m + 1)$  th sub-carrier of the  $(l + 1)$  th band, satisfying:

$$\sum_{l=0}^{L-1} \sum_{m=0}^{M-1} E_m^l = P_{in} \quad (9)$$

After the zero-forcing equalizer, the achievable total bit-rate of the  $(l + 1)$  th band can be calculate as:

$$C = \sum_{l=0}^{L-1} \sum_{m=0}^{M-1} \log_2 \left\{ 1 + \frac{L^{N/L} \cdot \sigma^2}{|H_{m+Ml}|^2 \cdot E_m^l} \cdot F \right\} \quad (10)$$

Where  $|H_{m+Ml}|$  and  $\sigma^2$  are the corresponding sub-channel magnitude response and the noise power respectively,  $F$  represents the performance gap between the channel capacity and the achievable bit rate for an uncoded M-QAM system, represented as:

$$F = \frac{2}{3} \left\{ \text{erfc}^{-1} \left( \sqrt{\frac{P_e}{2}} \right) \right\}^2 \quad (11)$$

Consequently, the total practical bit rate can be calculated as:

$$C_{total} = \sum_{l=1}^L C_l \quad (12)$$

Therefore, DMT and MPPSK signals can be combined to extend transmission services with different occupied frequency regions.

#### IV. RESULTS AND DISCUSSION

To evaluate and assess the performance of the proposed scheme over IM/DD SI-POF link, extensive theoretical simulations and experimental tests are conducted. The simulated transmission system is shown in Fig. 4 which both transmitter and receiver are based on the offline processing in MATLAB/SIMULINK. 10-bit precision is used in the digital-to-analog conversion (DAC) as well as 8-bit resolution is adopted in the analog-to-digital conversion (ADC) leading to negligible quantization noise. The working current of the resonant cavity light-emitting diodes (RC-LED) should be limited in a linear range in order to maintain a linear relationship between the input modulate current and output optical powers and avoid introducing the LED non-linearity to the system. Considering the usual low-cost commercially available RC-LED (FC300R-120<sup>TM</sup>), the electrical-to-optical conversion factor is 0.05 W/A and the appropriate bias current should be set to 10 mA. After a standard 50m PMMA SI-POF (ESKA<sup>TM</sup> Premier, 150 dB/km loss at 650 nm) transmission, the received optical signal is detected by use of a PIN diode (FC300P-120<sup>TM</sup>) with the responsivity of 0.3 A/W and captured by ADC components. Finally, digital signal processing is off-line implemented in MATLAB.

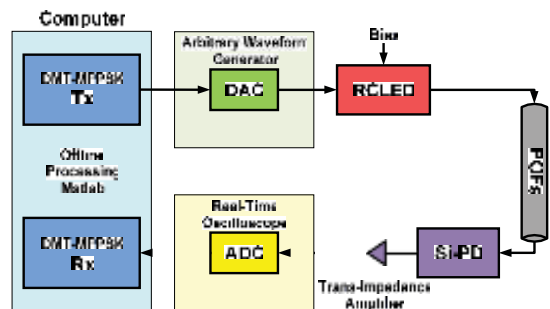


Fig. 4. The setup of POF transmission.

Before investigating the transmission performance, the number of sub-band of DMT should be firstly considered in order to calculate the optimal used bandwidth. Experiment is carried out to compare with these four systems: Conventional DMT, abbreviated as ‘‘C-DMT’’; One-band DFT-S DMT,

abbreviated as ‘‘SC’’; 4-band DFT-S DMT, abbreviated as ‘‘4-band’’; 8-band DFT-S DMT, abbreviated as ‘‘8-band’’. For fair comparison, all four systems own the fixed input power and same modulation parameters depicted as in Table 1. The sub-carrier number  $N$  is varied from 1 to 1024 and the fixed sub-carrier spacing is  $\Delta f = 0.488\text{MHz}$ . According to the received probing symbols, the channel estimation information is obtained and normalized noise power spectral density (PSD) is measured as -112 dB/Hz. The simplest sub-optimal Chow

algorithm with a target SER of  $1 \times 10^{-4}$  is employed since it is practical and effective in POF transmission.

TABLE I. MODULATION PARAMETERS

DMT	Parameters
Sampling frequency(GHz)	1
IFFT/FFT	4N
Subcarrier spacing (MHz)	0.488
Subcarrier number N	1~1024
Cyclic Prefix (CP) ratio	1/64

Fig. 5 shows the total achievable transmission rate of each system with respect to different used bandwidth. It can be seen clearly that each scheme can reach the maximal transmission rate with its optimal used bandwidth, 4-band and 8-band achieves similar performance. Moreover, the transmission rates of all DFT-S schemes outperform the C-DMT. MB-DFT-S owns the robustness ability against fiber nonlinearity besides the SC scheme whose transmission rate is sensitive to the bandwidth and the optimal range is limited only form 150 MHz to 200 MHz. Furthermore, the capacity performance of SC will be severely degraded once the used bandwidth beyond this optimal range. Fig. 6 shows the complementary cumulative distribution function (CCDF) performance of the four schemes, the C-DMT owns the highest PAPR whereas the SC obtains the lowest, the less the band splitted, the lower the PAPR we got. We know that the efficient PAPR reduction can benefit the SNR gain of the system. In order to make a good trade-off between transmission rate and PAPR performance, 4-band scheme is chosen in the following composite transmission.

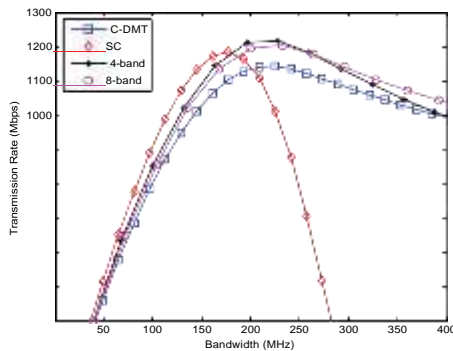


Fig. 5. Transmission rate of different system.

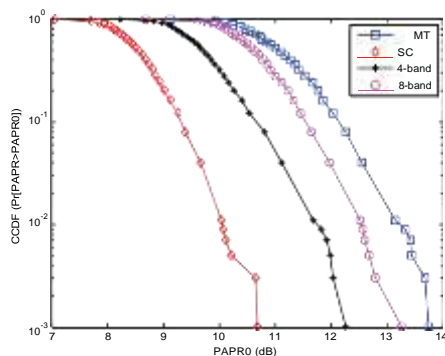


Fig. 6. PAPR performance of different system.

A DMT symbol containing 512 sub-carriers (the first sub-carrier is set to null) is random generated and 2048 points IFFT/FFT block is adopted. Hence, the cyclic prefix (CP) and each DMT symbols length can be fixed to  $0.032 \mu s$  and  $2.08 \mu s$  respectively. After the implementation of Chow algorithm, the calculated bits and power are allocated for each sub-carrier and shown in Fig. 7. The results demonstrate that the previous (2-484) sub-carriers, corresponding the frequency range between (0-236) MHz, is used to carry useful DMT data and the constant power allocation is performed for a group of sub-carrier with same constellation order. Additionally, no bits are allocated for the remaining which results in a low SNR and then reasonably arranged for MPPSK transmission. Two MPPSK channels are modulated by the carrier at 250 MHz and 260 MHz with the parameter as followings:  $N_0 = 70$ ,  $M_0 = 8$ ,  $K_0 = 4$ ,  $A_0 = 0$ ,  $B_0 = 3$  and  $O = n$ . Finally the composite 4-band DFT-S DMT and MPPSK signal with a total transmission rate of 1.122 Gbps is generated in the transmitter. The PSD of the hybrid transmission signal is shown in Fig. 8.

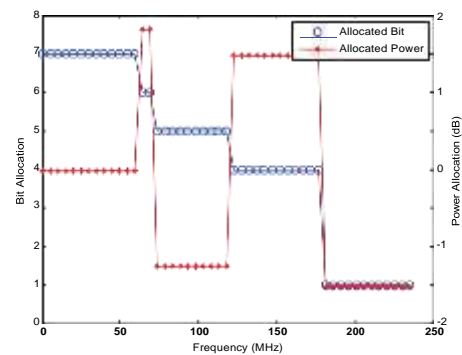


Fig. 7. Allocated bits and power.

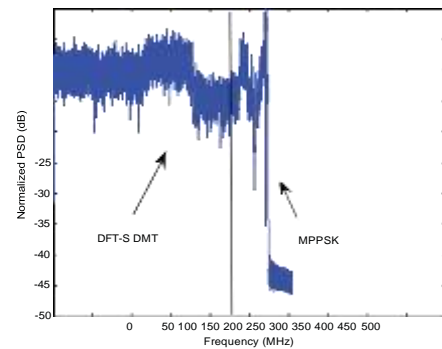


Fig. 8. PSD for the transmitted signal.

After 50m SI-POF link, the hybrid electrical signal from the photodetector is separated by the receiving filter into two parts distinguished by their occupied frequency bands. Then, the DMT signal can be demodulated by the particular approaches as the Fig. 3 shown and the constellation performance corresponding 32-QAM and 16-QAM is depicted in Fig. 9. It can be found that the concentrated constellation is beneficial for symbol discrimination which indicates the received signal quality is good after the equalization. Fig. 10 shows the

distinguishing envelope of two MPPSK channels after SIF processing and indicates that the low SNR of the DMT signal at high frequency regions introduce less interference to the MPPSK. Thus, the received symbols of MPPSK can be recovered with the help of a simple envelope detector as in [10]. Finally, the BER of  $1.2019 \times 10^{-4}$  and  $2.01 \times 10^{-3}$  for uncoded DMT and MPPSK is obtained which is suitable for reception with forward error correction (FEC). The results demonstrate that the composite signals in terms of DMT and MPPSK can maintain the coexistence transmission in their respective bands over SI-POF link.

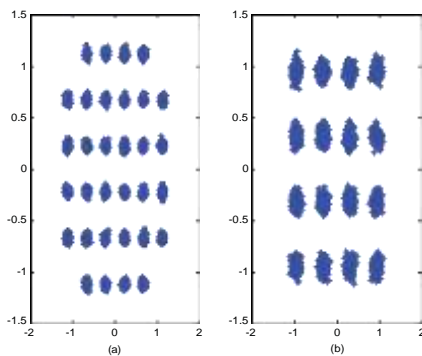


Fig. 9. Constellation diagrams (a) for 145-242 sub-carriers (b) for 243-363 sub-carriers

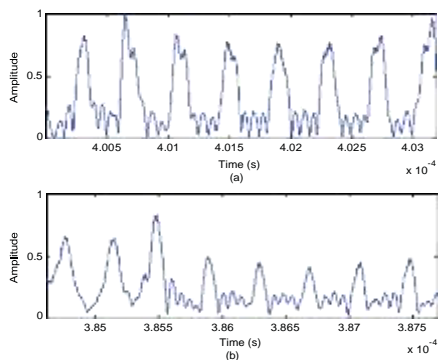


Fig. 10. Envelope for MPPSK signals (a) for the first branch (b) for the second branch

## V. CONCLUSION

Composite transmission over the IM/DD channel of SI-POF link is investigated and a novel modulation scheme with multiple services combining MB-DFT-S DMT and MPPSK is proposed. The new scheme takes advantage of Chow algorithm to realize an adaptive bit rate and maintain spectral coexistence in the low SNR regions. The transmission rate with different used bandwidth and the PAPR performance are investigated. Experiment results show that the MB-DFT-S scheme can achieve a higher transmission rate than the conventional DMT and more efficient in presence of non-linearity mitigation.

Furthermore, the optimal 4-band scheme is chosen in the converged DMT and MPPSK transmission over 50 m SI-POF. Finally, the data with total 1.122 Gbps are successfully transported over 50 m SI-POF and a good BER performance is obtained. The results present a fact that multiple services transmitting with DMT and MPPSK is suitable for POF based infrastructure in future home access networks.

## ACKNOWLEDGMENT

The author would like to thank B Madhu and Ravi for the insightful discussion and generous help.

## REFERENCES

- [1] Nespola A, Abrate S, Gaudino R, et al, "High-speed communications over polymer optical fibers for in-building cabling and home networking," *IEEE Photonics Journal*, vol. 2, No. 3, pp. 347-358, 2010.
- [2] Visani D, Shi Y, Okonkwo C M, et al, "Wired and wireless multi-service transmission over 1mm-core GI-POF for in-home networks," *Electronics Letters*, Vol. 47, No. 3, pp. 203-205, 2011.
- [3] Beltrán M, Shi Y, Okonkwo C, et al, "In-home networks integrating high-capacity DMT data and DVB-T over large-core GI-POF," *Optics express*, Vol. 20, No. 28, pp. 29769-29775, 2012.
- [4] Popov M, "The convergence of wired and wireless services delivery in access and home networks," *Optical Fiber Communication (OFC), collocated National Fiber Optic Engineers Conference, 2010 Conference on (OFC/NFOEC)*. IEEE, pp. 1-3, 2010.
- [5] Miao P, Wu L, Peng L, "A novel modulation scheme for short range polymer optical fiber communications," *Journal of Optics*, vol.15, no. 10, pp. 105407, 2013.
- [6] Peng L, Haese S, Hélarid M, "Optimized Discrete Multitone Communication Over Polymer Optical Fiber," *Journal of Optical Communications and Networking*, vol.5, no. 11, pp. 1313-1327, 2013.
- [7] Randel S, Breyer F, Lee S C J, et al, "Advanced modulation schemes for short-range optical communications," *IEEE Journal of Selected Topics in Quantum Electronics*, vol. 16, no. 5, pp. 1280-1289, 2010.
- [8] Armstrong J, "OFDM for optical communications," *Journal of lightwave technology*, vol. 27, no. 3, pp. 189-204, 2009.
- [9] Wu L N, "Advance in UNB high speed communications," *Prog. Nat. Sci.(in Chinese)*, vol. 17, pp. 143-149, 2007.
- [10] Miao P, Wu L, Jin Y, "On power spectrum optimization of M-ary position PSK modulations," *Journal of Electronics and Information Technology*, vol. 35, no. 7, pp. 1687-1693, 2013.
- [11] Peng L, Hélarid M, Haese S, "Optimization of multi-band DFT-spread DMT system for polymer optical fiber communications," *2013 IEEE International Conference on Communications (ICC)*, pp. 3862-3867, 2013.
- [12] Cárdenas D, Nespola A, Spalla P, et al, "A media converter prototype for 10-Mb/s ethernet transmission over 425 m of large-core step-index polymer optical fiber," *Journal of lightwave technology*, vol. 24, no. 12, pp. 4946-4952, 2006.
- [13] Peng L, Hélarid M, Haese S, "On Bit-loading for Discrete Multi-tone Transmission over Short Range POF Systems," *Journal of lightwave technology*, vol. 31, no. 24, pp. 4155-4165, 2013.
- [14] Shieh W, Tang Y, "Ultrahigh-speed signal transmission over nonlinear and dispersive fiber optic channel: The multicarrier advantage," *IEEE Photonics Journal*, vol. 2, no. 3, pp. 276-283, 2010.
- [15] Tang Y, Shieh W, Krongold B S, "DFT-spread OFDM for fiber nonlinearity mitigation," *IEEE Photonics Technology Letters*, vol. 22, no. 16, pp. 1250-1252, 2010.